Received: 6 January 2022 | Revised: 20 April 2022 | Accepted: 30 April 2022

DOI: 10.1111/cas.15391

Cancer Science WILEY

ORIGINAL ARTICLE

Opposing roles of HDAC6 in liver regeneration and hepatocarcinogenesis

Sophors Phorl[1] | Azra Memon[2] | Yuri Seo[1] | Thi Oanh Hoang[1] | Trung Nghia Tran[1] | Le Minh Tri Nguyen[1] | Chang Hoon Lee[3] | Woon Kyu Lee[2] | Joo-Yong Lee[1]

[1]Graduate School of Analytical Science and Technology, Chungnam National University, Daejeon, Korea

[2]Department of Biomedical Sciences, School of Medicine, Inha University, Incheon, Korea

[3]Center for Drug Platform Technology, Korea Research Institute of Chemical Technology, Daejeon, Korea

Correspondence
Woon Kyu Lee, Department of Biomedical Sciences, School of Medicine, Inha University, 100 inha-ro, Nam-gu, Incheon 22212, Korea.
Email: wklee@inha.ac.kr

Joo-Yong Lee, Graduate School of Analytical Science and Technology, Chungnam National University, 99 Daehak-ro(St), Yusoeng, Daejeon 305-764, Korea.
Email: leejooyong@cnu.ac.kr

Funding information
the Ministry of Health & Welfare, Republic of Korea, Grant/Award Number: HI21C1503; Ministry of Science and ICT, South Korea, Grant/Award Number: CNU(2021)-011; National Research Foundation of Korea, Grant/Award Number: 2016M3A9E1918314 and 2019R1A2C1005334

Abstract

Histone deacetylase 6 (HDAC6), a deacetylase of p53, has emerged as a privileged inhibitory target for cancer therapy because of its deacetylating activity for p53 at K120 and K373/382. However, intricate roles of HDAC6 in hepatocellular carcinogenesis have been suggested by recent evidence, namely that HDAC6 ablation suppresses innate immunity, which plays critical roles in tumor immunosurveillance and antitumor immune responses. Therefore, it is valuable to determine whether HDAC6 ablation inhibits hepatocellular carcinogenesis using in vivo animal models. Here, we firstly showed that HDAC6 ablation increased K320 acetylation of p53, known as pro-survival acetylation, in all tested animal models but did not always increase K120 and K373/382 acetylation of p53, known as pro-apoptotic acetylation. HDAC6 ablation induced cellular senescence in primary MEFs and inhibited cell proliferation in HepG2 cells and liver regeneration after two-thirds partial hepatectomy. However, the genetic ablation of HDAC6 did not inhibit hepatocarcinogenesis, but instead slightly enhanced it in two independent mouse models (DEN + HFD and DEN + TAA). Notably, HDAC6 ablation significantly promoted hepatocarcinogenesis in a multiple DEN treatment hepatocellular carcinoma (HCC) mouse model, mimicking chronic DNA damage in the liver, which correlated with hyperacetylation at K320 of p53 and a decrease in inflammatory cytokines and chemokines. Our data from three independent in vivo animal HCC models emphasize the importance of the complex roles of HDAC6 ablation in hepatocellular carcinogenesis, highlighting its immunosuppressive effects.

KEYWORDS
acetylation, HDAC6, hepatocellular carcinogenesis, innate immunity, p53

Abbreviations: DEN, diethylnitrosamine; HCC, hepatocellular carcinoma; HDAC6, histone deacetylase 6; HFD, high-fat diet; p53, tumor protein p53; PHx, hepatectomy; TAA, thioacetamide; MEF, mouse embryonic fibroblast; DAVID, Database for Annotation, Visualization and Integrated Discovery.

Sophors Phorl and Azra Memon contributed equally to this work.

1 | INTRODUCTION

The liver performs many essential roles, from early fetal hematopoiesis through metabolic regulation of dietary nutrients to adult homeostasis.[1] Among liver diseases, hepatocellular carcinoma (HCC) is the fifth most common malignancy and the second most common cause of cancer-associated mortality worldwide.[2] Hepatocellular carcinoma typically develops in patients with chronic liver diseases, such as viral hepatitis, nonalcoholic fatty liver disease, and alcoholic liver disease.[3] Chronic liver injury triggers permanent hepatocellular damage, hepatocyte (HC) regeneration, and inflammation, and has been widely accepted as the unifying principle that promotes hepatocellular carcinogenesis.[4] Based on this principle, several mouse models of HCC have been developed that utilize diethylnitrosamine (DEN), a carcinogen that induces DNA damage and tumor formation.[5,6]

Upon various stresses in liver, the tumor suppressor p53 plays a central role in multiple biological processes, including DNA damage repair, cell cycle arrest, apoptosis, and senescence.[7] As the "guardian of the genome," it has been widely accepted that the activation of p53 is critical to suppress cancer development.[8] More than 300 different post-translational modifications of p53 have been reported and have been shown to be crucial for regulating its tumor-suppressive functions.[7] Among them, p53 acetylation has recently been highlighted and shown to control its transcriptional activity, selection of growth-inhibitory versus apoptotic gene targets, and biological consequences in response to various cellular stresses.[7] However, the importance of p53 acetylation in HCC has not been sufficiently investigated using in vivo evidence from mouse models.

Histone deacetylase 6 (HDAC6) is a specific deacetylase of p53.[9,10] Genetic ablation of HDAC6 increases K120 acetylation of p53, resulting in mitochondrial dysfunction and apoptosis in mouse mesenchymal stem cells.[9] In addition, the pharmaceutical selective inhibition of HDAC6 increases p53 acetylation at lysine 381/382 (K381/382), which stabilizes and activates p53, resulting in an anticancer effect.[11] Interestingly, Ding et al reported that HDAC6 promotes cell growth by inhibiting p53 transcriptional activity in the HepG2 cell line.[10] Notably, the mRNA and protein levels of HDAC6 are upregulated in HCC tissues.[10] In addition, HDAC6 can participate in tumorigenesis and development through various pathways, such as oncogenic transformation, migration, invasion, and anticancer immunity.[12] Although accumulating in vitro evidence indicates that HDAC6 could be a potential therapeutic target against cancer, the physiological roles of HDAC6 in HCC remain to be elucidated with support from in vivo evidence from mouse models.

In this study, we investigated the role of HDAC6 in HCC related to the acetylation status of p53 at lysine 120, 320, and 373/382 residues. In contrast to the general assumption that HDAC6 inhibition leads to p53 hyperacetylation, resulting in tumor suppression, our data from in vivo mice models emphasize the importance of the multiple roles of HDAC6 in HCC, highlighting its immunosuppressive effects.

2 | MATERIALS AND METHODS

The materials and methods used in this study are described in the "Supplementary Methods" in Appendix S1.

Data are shown as the mean ± standard error (SEM). Significance was calculated with Student's *t* test using GraphPad Prism version 9.2.0 (GraphPad Software). Statistical significance was set at $^{*}p < 0.05$, $^{**}p < 0.01$, and $^{***}p < 0.005$.

3 | RESULTS

3.1 | Histone deacetylase 6 deacetylates p53 at K120 and K320 residues related to cellular senescence

Histone deacetylase 6 has been reported as a p53 deacetylase at acetyl-K120[13] and at acetyl-K373/382 induced by the HDAC inhibitor trichostatin A[14]; however, the role of HDAC6 in p53 deacetylation at acetyl-K320 is not clear. Using primary MEFs from wild-type ($HDAC6^{+/y}$) and HDAC6 knockout ($HDAC6^{-/y}$) mice, we tested whether HDAC6 depletion induces spontaneous senescence during serial passaging. Hence, we performed a SA-β-Gal staining assay to detect senescent MEFs at passage 11 after primary cell preparation. As shown in Figure 1A,B, $HDAC6^{-/y}$ MEFs included 42% SA-β-gal–positive senescent cells, but $HDAC6^{+/y}$ MEFs included only 22% of the same, indicating that HDAC6 expression inhibits cellular senescence. p21 is a well-known downstream regulator of p53-dependent cellular senescence. As shown in Figure 1C,D, both mRNA and protein levels of p21 were significantly increased in $HDAC6^{-/y}$ MEFs, which correlated with the acetylation at K120 and K320 of p53.

3.2 | Histone deacetylase 6 deacetylates ablation-induced p53-dependent p21 expression, inhibiting cell growth in HepG2 cells

To address the importance of HDAC6-dependent p53 deacetylation, we investigated the role of HDAC6 in the proliferation of HCC cells (HepG2). HepG2 cells were transfected with control and three independent HDAC6-specific siRNAs and subjected to MTT assay at the indicated times (24, 48, and 72 hours after transfection). As shown in Figure 2A, all three independent HDAC6-specific siRNA transfections significantly inhibited HepG2 cell proliferation. Western blot analysis showed that HepG2 cells have an intrinsically high level of acetyl-K120 p53 that was not further induced by HDAC6 knockdown (Figure 2B). In contrast, the level of acetyl-K320 p53 was greatly increased by all three independent HDAC6-specific siRNAs (Figure 2B). Importantly, the protein level of p21 was strongly correlated with the level of acetyl-K320 p53. To further confirm p53-dependent p21 induction in HDAC6-knockdown HepG2 cells, we knocked down HDAC6 and p53 in HepG2 cells. As

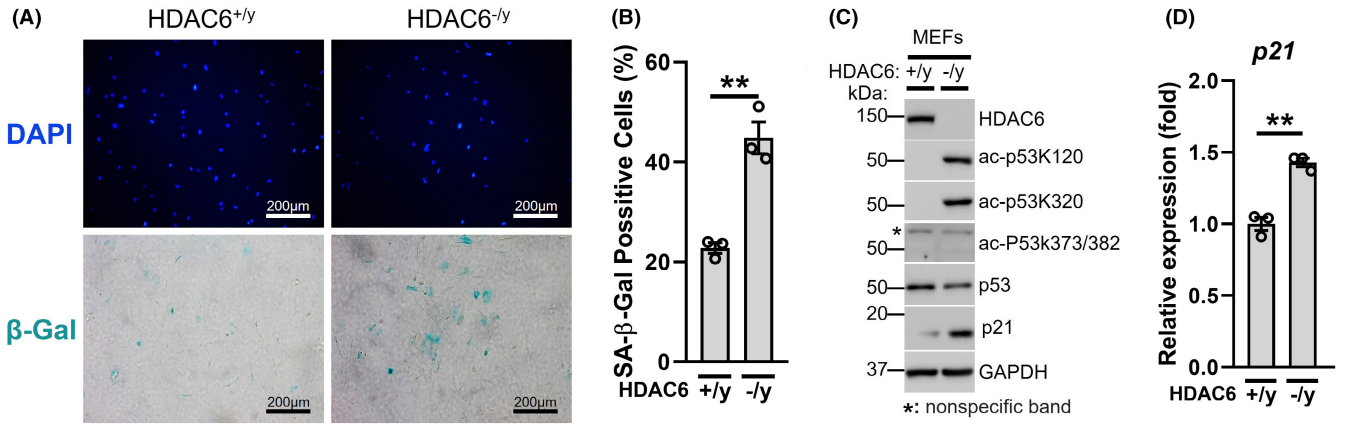

FIGURE 1 Loss of histone deacetylase 6 (HDAC6), induces p53 acetylation and senescence in primary MEFs. (A), Primary HDAC6$^{+/y}$ and HDAC6$^{-/y}$ MEFs were subjected to SA-β-gal and DAPI staining, at passage 11. (B), A percentage of SA-β-gal–positive cells to total cell numbers ($n = 3$). (C), The sample from (A) was subject to Western blot for HDAC6, p53, acetylated p53 (K320, K120, and K373/382), p21, and GAPDH (asterisk, nonspecific band). (D), qRT-PCR analysis of p21 mRNA expression ($n = 3$) from MEFs as described in (A)

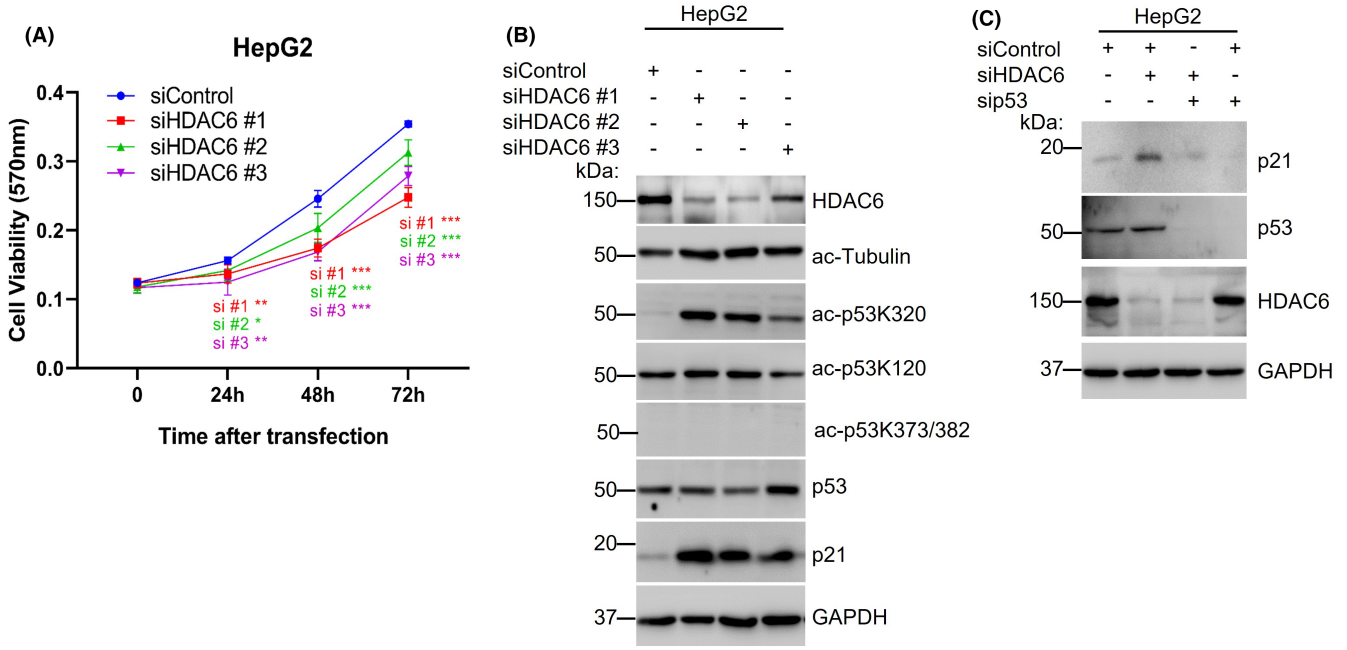

FIGURE 2 Histone deacetylase 6 (HDAC6) knockdown in HepG2 induces p53 acetylation and inhibits cell growth. A-B, HepG2 cells were transfected with three independent HDAC6 siRNAs. (A), MTT assay analysis to quantify cell viability ($n = 4$ per group). (B), Western blot analysis of HDAC6, p53, acetylated p53 (K320, K120, and K373/382), p21, and GAPDH at 48 h after transfection. (C), HepG2 cells were cotransfected with HDAC6 and p53 siRNA, and subjected to Western blot for p21, p53, HDAC6, and GAPDH

shown in Figure 2C, HDAC6 knockdown increased p21 expression, which was completely reversed by HDAC6/p53 double knockdown.

3.3 | Genetic ablation of HDAC6 inhibits HC proliferation after PHx

To investigate the physiological role of HDAC6 in liver regeneration, we performed two-thirds PHx in both HDAC6$^{+/y}$ and HDAC6$^{-/y}$ mice (Figure 3A) and subsequently collected sera and liver tissues at the indicated time points. The liver to body weight ratio was largely decreased at 24 hours after PHx and gradually recovered but did not show significant differences between HDAC6$^{+/y}$ and HDAC6$^{-/y}$ mice (Figure 3B). Serum albumin levels were reduced at 24 hours post PHx, but no significant difference was observed between HDAC6$^{+/y}$ and HDAC6$^{-/y}$ mice (Figure S1A). We did not observe significant changes in serum alkaline phosphatase (ALP) levels in any of the samples (Figure S1B). Serum aspartate aminotransferase (AST) and alanine aminotransferase (ALT) levels were significantly increased at 24 hours post PHx, but no significant differences were observed between HDAC6$^{+/y}$ and HDAC6$^{-/y}$ mice (Figure S1C,D). The liver tissues of HDAC6$^{+/y}$ and HDAC6$^{-/y}$ mice exhibited neither necrosis

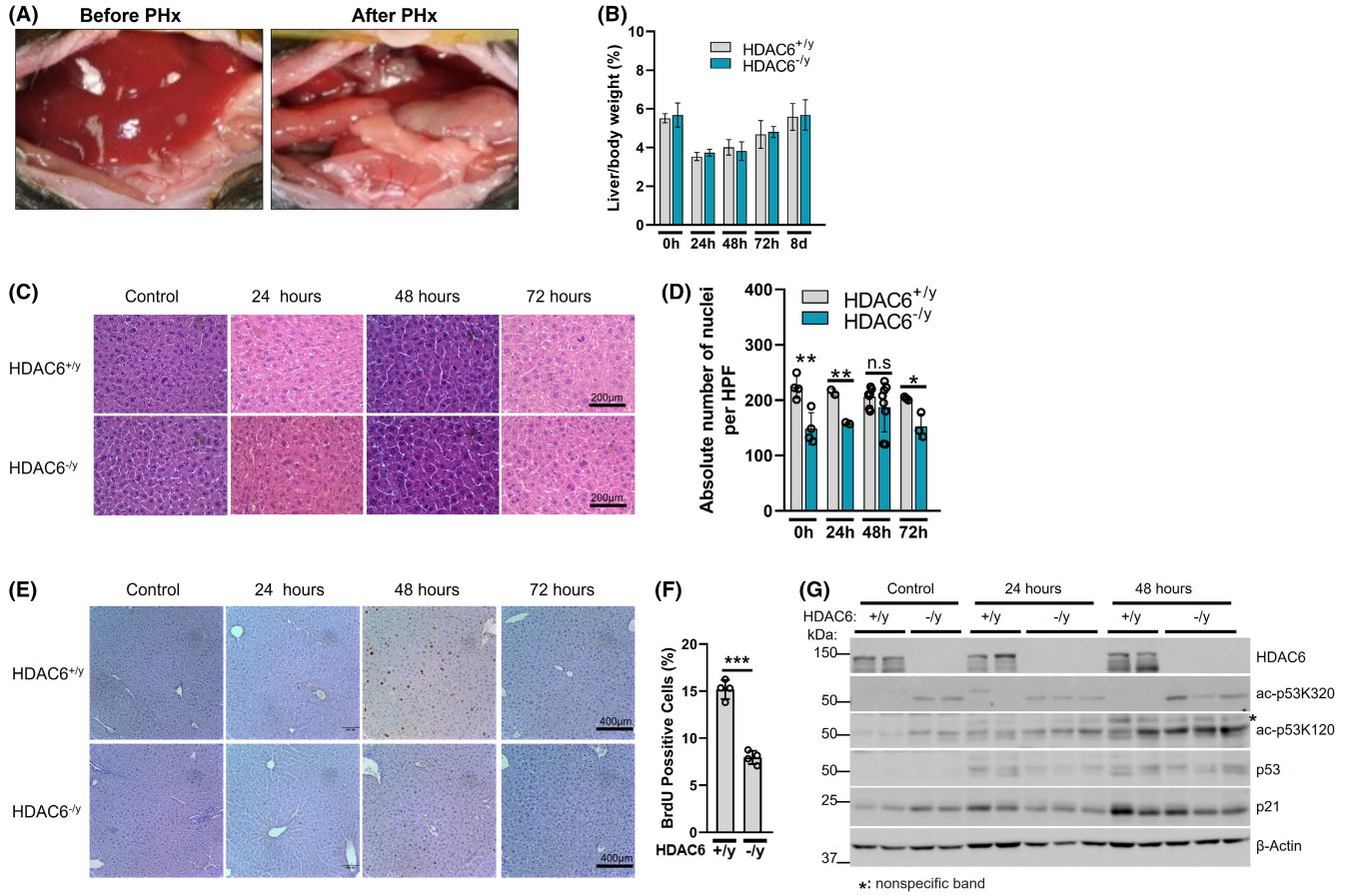

FIGURE 3 Loss of histone deacetylase 6 (HDAC6) inhibits hepatocyte proliferation after two-thirds hepatectomy (PHx). (A), Photographs of the resected surface of livers during PHx. (B), Liver to body weight ratio after PHx. (C), H&E staining of control and regenerative livers after PHx. (D), The number of hepatocyte nuclei per high-power field. (E), BrdU incorporation assay after PHx. (F), Percentage of BrdU-positive hepatocytes after PHx ($n = 4$ per group). (G), Western blot analysis of HDAC6, p53, Ac-p53K320, p21, and β-actin in liver (asterisk, nonspecific band)

nor inflammation after PHx, as analyzed by hematoxylin and eosin (H&E) staining (Figure 3C). Notably, the number of HC nuclei per high-power field was significantly reduced in all HDAC6$^{-/y}$ mouse liver samples, except at 48 hours after PHx (Figure 3D), suggesting that HC cell size is increased by genetic ablation of HDAC6. In response to PHx, HC proliferation increased in HDAC6$^{+/y}$ mice at 48 hours after PHx, as assessed by the incorporation of bromodeoxyuridine (BrdU). This proliferative response of HCs was significantly reduced by ~52% in HDAC6$^{-/y}$ mice at 48 hours after PHx (Figure 3E,F). Notably, a significant amount (about 80%) of HCs are polyploid (>4n) in normal mouse liver.[15] Thus, it is plausible if polyploidy of HCs is increased in HDAC6$^{-/y}$ liver, which would explain nonreplicative liver regeneration in HDAC6 liver after PHx. To address it, we isolated HCs and checked DNA contents by FACS analysis. Interestingly, polyploidy (4C, >8C) was increased in isolated HCs from HDAC6$^{-/y}$ liver (Figure S2).

To address the role of HDAC6 in p53 deacetylation and subsequent p21 induction upon liver regeneration, we measured the protein levels of HDAC6, p21, acetyl-K120, -K320, and total p53. Protein levels of p21 and p53 in both HDAC6$^{+/y}$ and HDAC6$^{-/y}$ mice increased after PHx treatment. Although protein levels of p21 in HDAC6$^{-/y}$ mice were slightly increased before PHx, these levels did not differ significantly between HDAC6$^{+/y}$ and HDAC6$^{-/y}$ mice at 24 and 48 hours after PHx (Figure 3G). Consistently, protein levels of acetyl-K320 p53 were increased in all HDAC6$^{-/y}$ mice compared with those in HDAC6$^{+/y}$ mice. Notably, the protein levels of acetyl-K120 p53 in both HDAC6$^{+/y}$ and HDAC6$^{-/y}$ mice increased after PHx, as did the total protein level of p53. An increase in acetyl-K120 p53 in HDAC6$^{-/y}$ mice was detected before PHx, and the difference in its level between HDAC6$^{+/y}$ and HDAC6$^{-/y}$ mice was reduced after PHx.

3.4 | Histone deacetylase 6 ablation did not inhibit HCC in the DEN + HFD model

To test whether whole-body HDAC6 ablation inhibits HCC development in mice, we injected HDAC6$^{+/y}$ and HDAC6$^{-/y}$ mice at 2 weeks of age with 25 mg/kg of the hepatic carcinogen DEN and fed them with a high-fat diet (HFD) as a tumor promoter, following a previously described protocol that recreates HCC under obesity conditions (Figure 4A).[16] Surprisingly, whole-body HDAC6 knockout did not

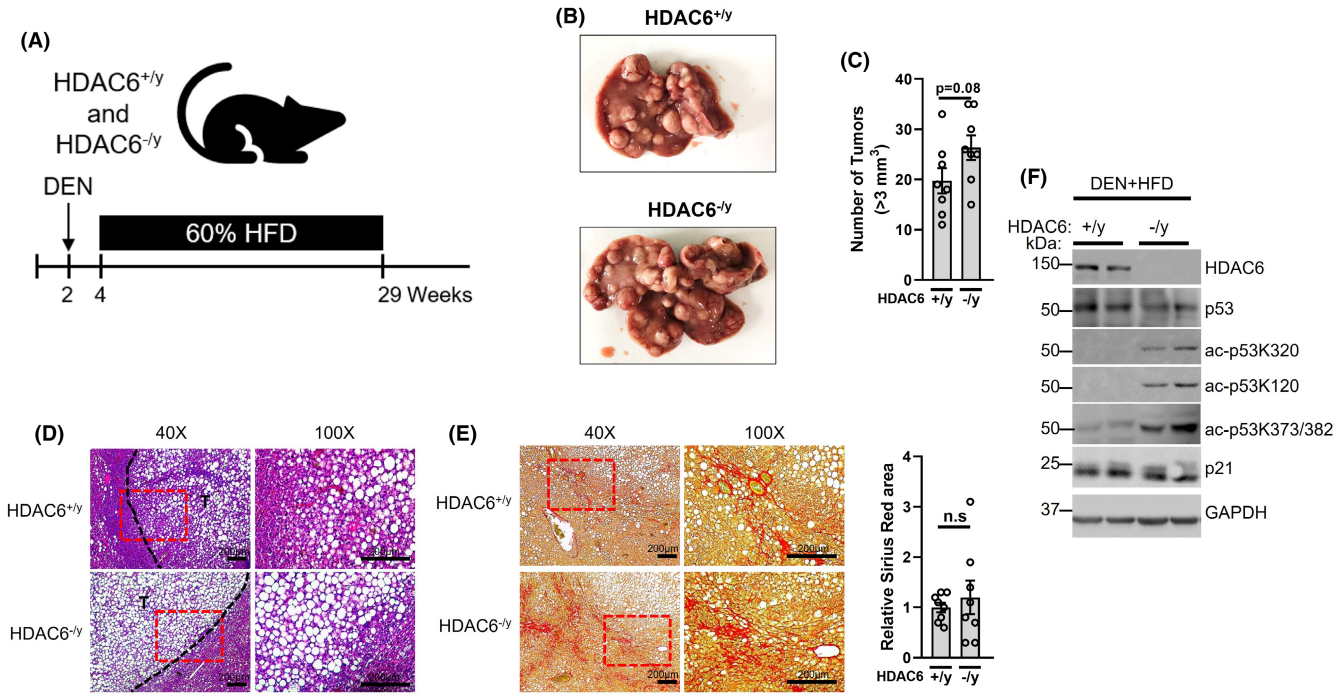

FIGURE 4 Effect of histone deacetylase 6 (HDAC6) deficiency in the diethylnitrosamine (DEN) + high-fat diet (HFD)–induced hepatocellular carcinoma (HCC) model. (A), Schematic representation of DEN + HFD–induced HCC protocol. (B), Representative images of livers from HDAC6$^{+/y}$ and HDAC6$^{-/y}$ mice treated as in (A). (C), The number of tumors (>3 mm^3) in HDAC6$^{+/y}$ and HDAC6$^{-/y}$ livers. (n = 8 per group). D, H&E staining of HDAC6$^{+/y}$ and HDAC6$^{-/y}$ livers treated as in (A) (T, tumor; black dotted line, separate tumor and normal tissues; red dotted line, region of the field magnified). E, Sirius Red staining of HDAC6$^{+/y}$ and HDAC6$^{-/y}$ livers treated as in (A) (red dotted line, region of the field magnified). F, Quantification of the Sirius Red–positive area from (E) (n = 8 per group). G, Western blot for HDAC6, p21, p53, acetylated p53 (K320, K120, and K373/382), and GAPDH (n = 2 per genotype)

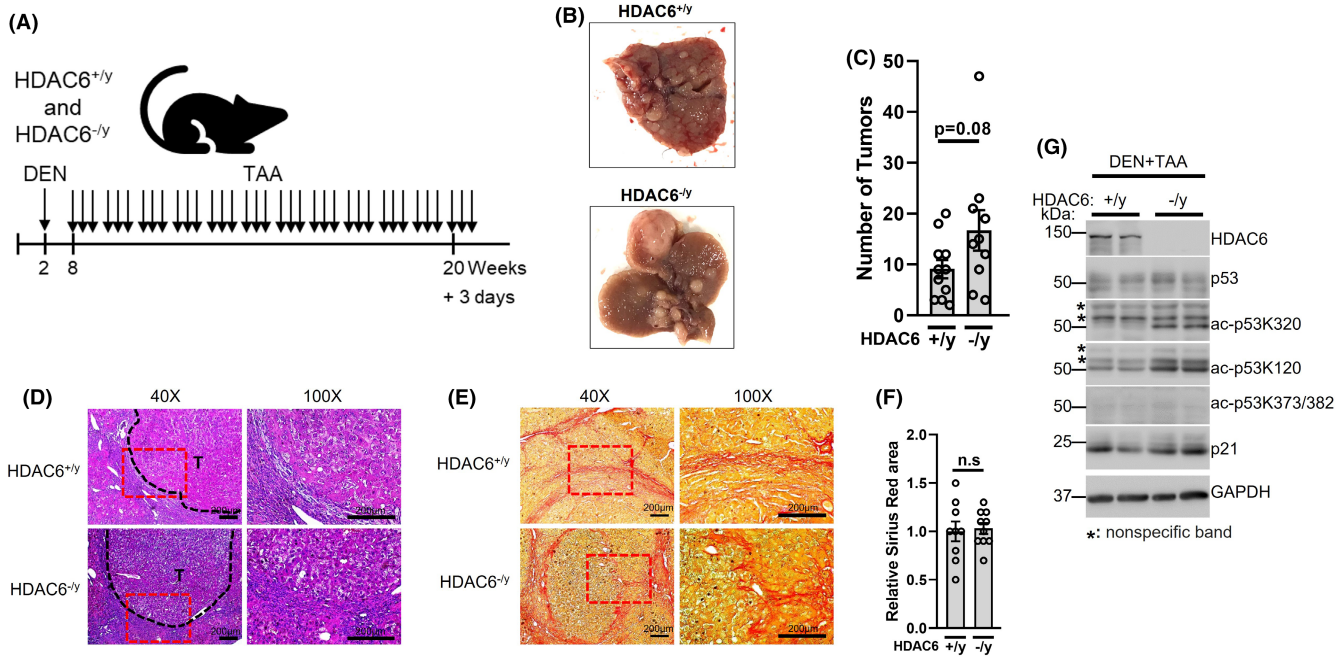

FIGURE 5 Effect of histone deacetylase 6 (HDAC6) deficiency in the (diethylnitrosamine) DEN + (thioacetamide) TAA–induced hepatocellular carcinoma (HCC) model. (A), Schematic representation of the DEN + TAA–induced HCC protocol. (B), Representative images of livers from HDAC6$^{+/y}$ and HDAC6$^{-/y}$ mice treated as in (A). (C), The total number of tumors in HDAC6$^{+/y}$ and HDAC6$^{-/y}$ livers (n = 10-11 per group). (D), H&E staining of HDAC6$^{+/y}$ and HDAC6$^{-/y}$ livers after DEN + TAA treatment (T, tumor; black dotted line, separate tumor and normal tissues; red dotted line, region of the field magnified). (E), Sirius Red staining of HDAC6$^{+/y}$ and HDAC6$^{-/y}$ livers after DEN + TAA (red dotted line, region of the field magnified). (F), Quantification of the Sirius Red–positive area from (E) (n = 8 per group). (G), Western blot to check levels of HDAC6, p21, p53, acetylated p53 (K320, K120, and K373/382), and GAPDH (asterisk, nonspecific band)

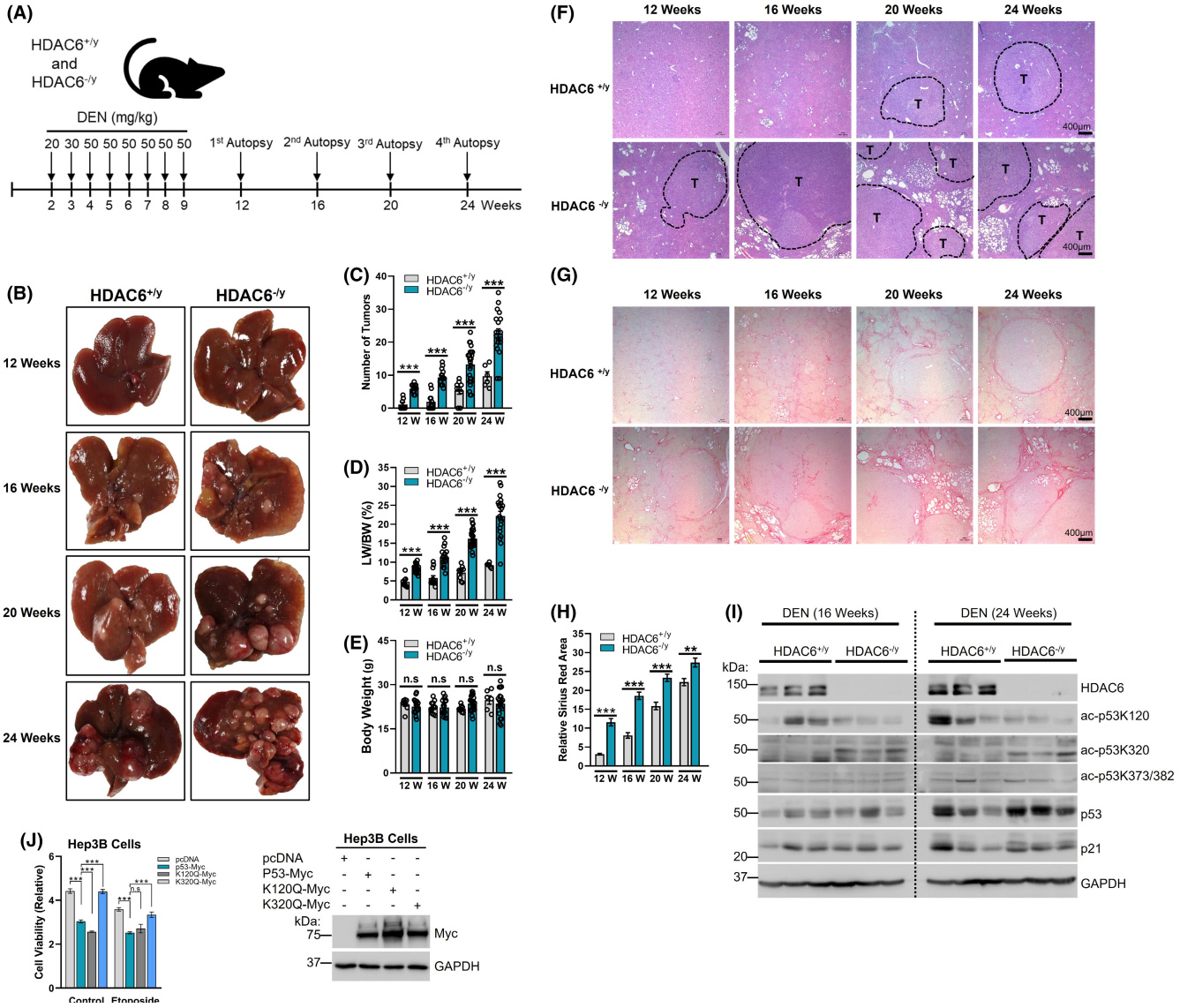

FIGURE 6 Effect of histone deacetylase 6 (HDAC6) deficiency in the multiple diethylnitrosamine (DEN) treatment hepatocellular carcinoma (HCC) model. (A), Schematic representation of the multiple DEN treatment–induced HCC protocol. (B), Representative images of livers from HDAC6$^{+/y}$ and HDAC6$^{-/y}$ mice treated as in (A). (C), Total number of tumors, (D) liver to body ratio, and (E) body weight in HDAC6$^{+/y}$ and HDAC6$^{-/y}$ mouse. C-E, n = 4-25 per group (the circle dots in graphs represent mouse numbers). (F), H&E staining of HDAC6$^{+/y}$ and HDAC6$^{-/y}$ livers (T, tumor; black dotted line, separate tumor and normal tissues). (G), Sirius Red staining of HDAC6$^{+/y}$ and HDAC6$^{-/y}$ livers. (H), Quantification of the Sirius Red–positive area from (G) n = 21-25 images per group. (I), Western blot for HDAC6, p21, p53, acetylated p53 (K320, K120, and K373/382), and GAPDH. (J), Hep3B cells were transfected with indicated protein expression plasmids. After 24 h of transfection, cells were treated with 30 μM etoposide for 24 h. Cell viability was measured by MTT assay (n = 4 per group). Ectopic expression of p53 was confirmed by Western blotting of anti-MYC and anti-GAPDH antibodies in the right panel

inhibit HCC and instead moderately enhanced its development, although this was not statistically significant (Figure 4B,C). Histological analysis of both genotypes revealed characteristics similar to those of human steatohepatitis HCC (Figure 4D), ballooning cancer cells, and liver fibrosis, which are typical of nonalcoholic steatohepatitis–related HCC.[17] Fibrosis was quantified using Sirius Red area analysis (Figure 4E). The severity of fibrosis was not changed by the genetic ablation of HDAC6 (Figure 4E,F). Protein levels of acetyl-K120 and -K320 p53 were higher in HDAC6$^{-/y}$ mice than in HDAC6$^{+/y}$ mice in the DEN + HFD HCC model (Figure 4G). Notably, the level of acetyl-K373/382 p53 was also increased in HDAC6$^{-/y}$ mice compared with that in HDAC6$^{+/y}$ mice in the DEN-HFD HCC model (Figure 4G). However, the protein levels of p21 were not changed by HDAC6 expression (Figure 4G).

3.5 | Histone deacetylase 6 ablation did not inhibit HCC in the DEN + TAA model

To further investigate the physiological roles of HDAC6 in HCC development, we adopted another mouse HCC model using DEN + TAA. Thioacetamide is a potent inducer of liver injury and

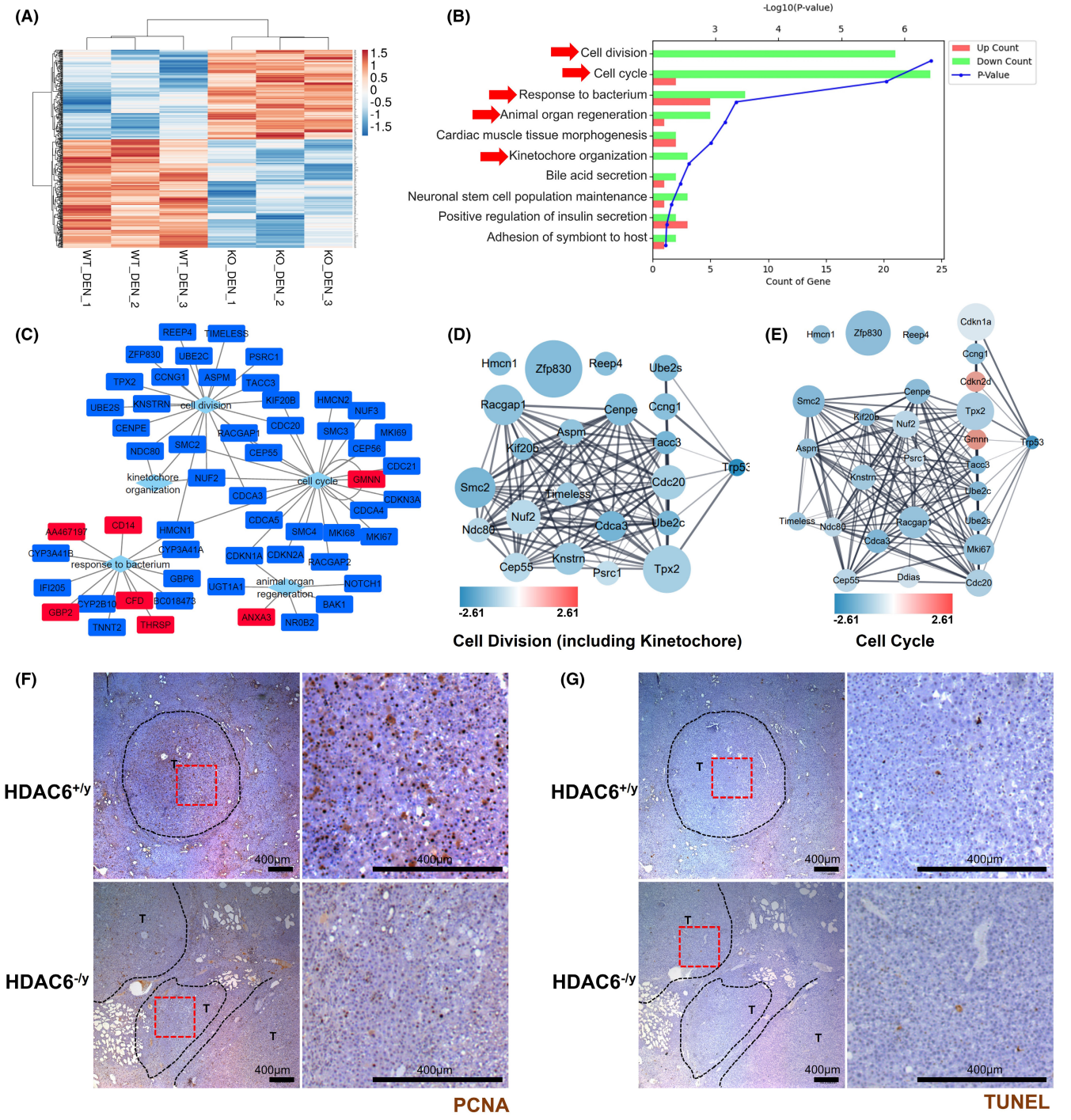

FIGURE 7 Histone deacetylase 6 (HDAC6) deficiency downregulates genes in cell cycle and cell division pathways. A, Heat map showing the clustering of mRNA expression profiles of bulk RNA-seq data from multiple diethylnitrosamine (DEN)–treated 12-week-old mice based on normalized mRNA expression level (fold change > 1.5, $p < 0.05$). B, Gene Ontology (GO) analysis performed with differentially expressed 341 genes in (A) using DAVID. Red arrows indicate GO pathway term used in (C). C, Selected GO pathway term gene network (red, upregulated genes; blue, downregulated genes). D-E, Gene-to-gene networks between p53 and groups of identified genes from the Cell Division and Cell Cycle GO terms in (C). Node color represents the degree of fold change (Log2 FC), and node size indicates *P* value (–Log10 *P* value). F, Proliferating cell nuclear antigen (PCNA) staining and (G) TUNEL staining of multiple DEN–treated mice at 24 weeks old. T, tumor; black dotted line, separate tumor and normal tissues; red dotted line, region of the field magnified

fibrosis that facilitates premalignant transformation in HCs. We injected 2-week-old male HDAC6$^{+/y}$ and HDAC6$^{-/y}$ mice with 25 mg/kg of DEN; at 8 weeks of age, these mice were injected with TAA (dissolved in 0.9% NaCl) thrice weekly for 12 weeks at increasing concentrations (first dose: 50 mg/kg; second dose: 100 mg/kg; third to sixth doses: 200 mg/kg; all subsequent doses: 300 mg/kg)

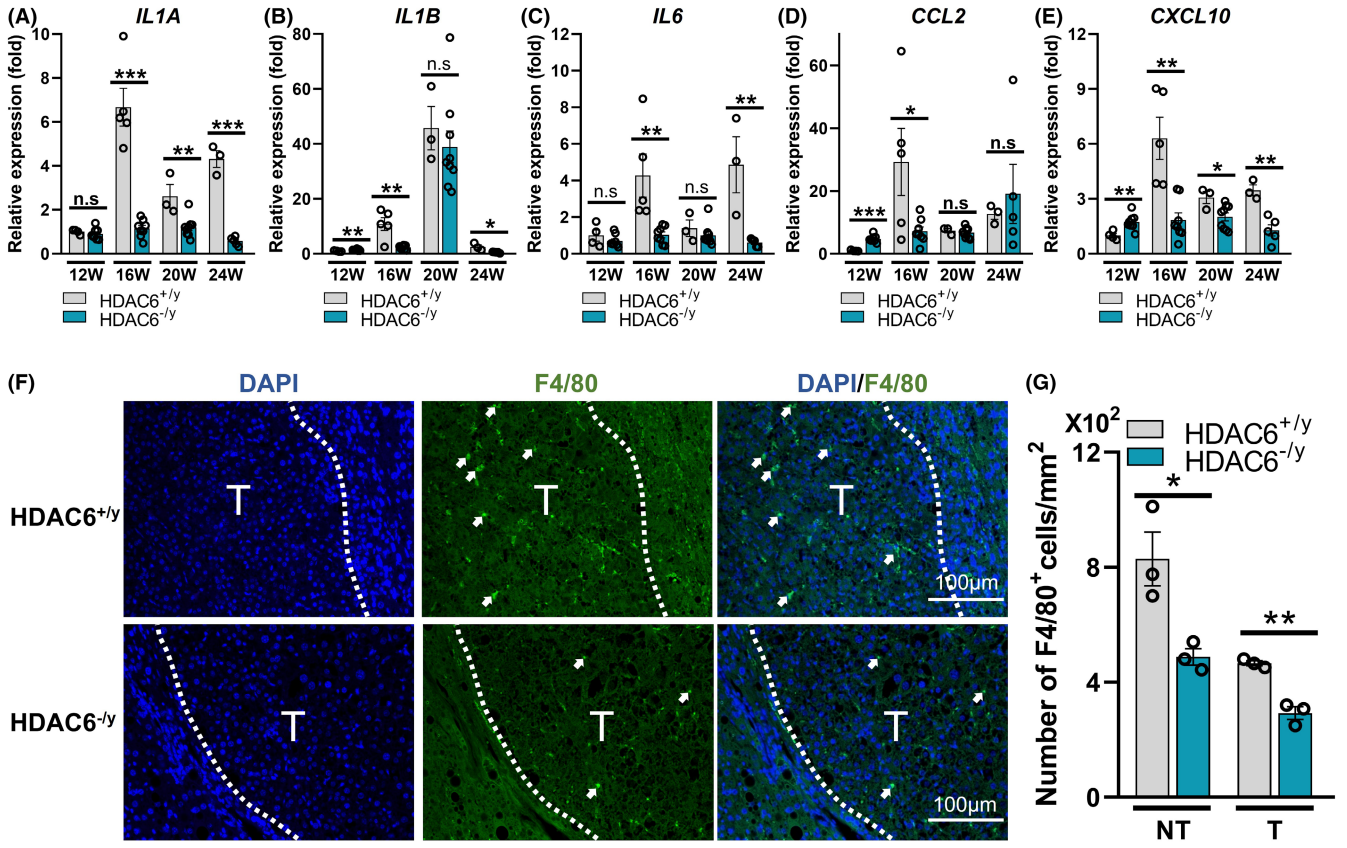

FIGURE 8 Histone deacetylase 6 (HDAC6) deficiency reduces innate immune response in the multiple diethylnitrosamine (DEN) treatment hepatocellular carcinoma (HCC) model. A-E, Total RNA isolated from the livers of each treatment group was subjected to qPCR analysis for mRNA expression of indicated genes. Data were calculated as fold change in 12-week DEN-treated HDAC6$^{+/y}$ livers using the $\Delta\Delta C_T$ method (n = 3-9 per group). F, Immunofluorescence analysis of liver tissue sections from 24-week-old mice with multiple DEN treatments using anti-F4/80 antibody for macrophages (green) and DAPI (blue) (NT, nontumor; T, tumor; white dotted line, separate tumor and normal tissues). G, Quantification of F4/80-positive cells from (F). (n = 3 per group)

(Figure 5A). Consistent with the DEN + HFD model, whole-body HDAC6 knockout did not inhibit HCC and instead moderately enhanced its development, although this was not statistically significant (Figure 5B,C). Histological analysis of both genotypes revealed characteristics similar to those of human adenoma HCC (Figure 5D). Fibrosis was quantified using Sirius Red area analysis (Figure 5E). The severity of fibrosis was not changed by the genetic ablation of HDAC6 (Figure 5E,F). Protein levels of acetyl-K120 and -K320 p53 were increased in HDAC6$^{-/y}$ mice compared with those in HDAC6$^{+/y}$ mice in the DEN + HFD HCC model (Figure 4G). However, p21 protein levels were not affected by the genetic ablation of HDAC6 (Figure 5G). Of note, acetyl-K373/382 p53 was not detected in either HDAC6$^{+/y}$ or HDAC6$^{-/y}$ mice in the DEN + TAA HCC model (Figure 5G).

3.6 | Global HDAC6 loss promotes HCC in multiple DEN treatment model of HCC

To investigate the roles of HDAC6 in HCC development, we adopted a simple one-stage HCC model using only DEN treatment. In total, eight doses of DEN were administered to HDAC6$^{+/y}$ and HDAC6$^{-/y}$ mice: the first dose of DEN was 20 mg/kg, the second dose was 30 mg/kg, and the next six doses were 50 mg/kg (Figure 6A), as previously reported[18]; mice were sacrificed at 12, 16, 20, and 24 weeks old with multiple DEN treatments. In contrast to the DEN + HFD and DEN + TAA HCC models, in this model, whole-body HDAC6 knockout significantly enhanced HCC development (Figure 6B–D). Compared with HDAC6$^{+/y}$ mice, HDAC6$^{-/y}$ mice that were administered multiple DEN treatments had significantly more tumors per liver (Figure 6C) and a larger liver to body weight ratio (Figure 6D). Animal weights did not differ throughout the study (Figure 6E). Histological analysis of both genotypes revealed characteristics similar to those of human adenoma HCC (Figure 6F). Fibrosis was quantified using Sirius Red staining analysis (Figure 6G,H). Histone deacetylase 6ablation led to increased fibrosis and steatosis, which were mainly outside the tumor area (Figure 6F–H).

To examine the protein levels of acetyl-p53 (K120, K320, and K373/382), p53, p21, HDAC6, and actin, we performed a Western blot analysis of liver lysates at 16 and 24 weeks old with multiple DEN treatments. Consistent with previous findings, protein levels of acetyl-K320 p53 were higher in HDAC6$^{-/y}$ mice than in HDAC6$^{+/y}$

mice (Figure 6I), and p21 protein levels were not affected by the genetic ablation of HDAC6 in the multiple DEN treatment model of HCC (Figure 6I). Notably, the level of acetyl-K120 p53 was reduced in HDAC6$^{-/y}$ livers, and there were no differences in acetyl-K373/382 p53 levels between HDAC6$^{-/y}$ and HDAC6$^{+/y}$ mice (Figure 6I). To investigate the role of p53 acetylation on K120 and K320, we transfected wild-type and acetylation mimic mutants (K120Q and K320Q) of p53 into Hep3B cells lacking endogenous p53 expression. As shown in Figure 6J, wild-type and K120Q mutant p53 significantly reduced cell viability, but K320Q mutant p53 did not, under normal growth conditions and after 30 μM etoposide (a DNA-damaging reagent) treatment.

3.7 | Genetic ablation of HDAC6 inhibits the proliferation of HCC cells in multiple DEN treatment model of HCC

To search relevant genes and pathways with HCC, we performed QuantSeq 3′ mRNA sequencing with liver samples from 12-week-old wild-type (WT, $n = 3$) and HDAC6 knockout (KO, $n = 3$) mice with multiple DEN treatment and analyzed transcriptome. We selected 341 genes based on fold change greater than 1.5 and a P value less than 0.05 (Table S1) and performed unsupervised clustering. Two major clusters emerged as expected: WT and KO group (Figure 7A). Accordingly, principal component analysis (PCA) showed successful transcriptomic reprogramming in the KO group away from the WT group (Figure S3A). For further analysis, transcriptome data were submitted to DAVID-based Gene Ontology (GO) analysis, and the top 10 enriched GO terms are listed in Figure 7B. Among them, we selected five GO terms (red arrow indicated in Figure 7B) and drew the network with gene names with red (upregulated in KO) and blue (downregulated in KO) color (Figure 7C). Gene network analysis using STRING database showed that p53 is a critical regulator of cell division (including kinetochore organization), cell cycle, and animal organ regeneration (Figure 7D,E and Figure S3B), and almost all related genes were significantly downregulated in HDAC6$^{-/y}$ liver samples (Figure 7C), suggesting HCC proliferation defect in HDAC6 KO mice.

To investigate the role of HDAC6 in HCC cell proliferation and apoptosis in vivo, we performed proliferating cell nuclear antigen (PCNA) and TUNEL staining with wild-type and HDAC6$^{-/y}$ liver at 24 weeks with multiple DEN treatments. The conclusion of cell cycle inhibition from transcriptome analysis was further supported by a decreased number of PCNA-positive cells in HDAC6$^{-/y}$ liver at 24 weeks with multiple DEN treatments (Figure 7F). In contrast, we could not find a significant change in apoptosis-related genes in transcriptome analysis (Figure 7B) and the number of apoptotic cells in the TUNEL assay (Figure 7G). Despite a reduced number of proliferating cells in HDAC6$^{-/y}$ liver after DEN treatment (Figure 7F), the size and number of tumor nodules are significantly increased in HDAC6$^{-/y}$ liver after multiple DEN treatments (Figure 6B-E), which implies other regulatory mechanisms.

3.8 | Global HDAC6 loss suppresses immune activation in the multiple DEN treatment model of HCC

It was reported that genetic ablation or pharmaceutical inhibition of HDAC6 suppresses immune activation at multiple levels.[19–21] Thus, it is plausible that HDAC6 ablation inhibits immune activation, resulting in HCC outgrowth in multiple DEN–treated HCC models. To investigate the role of HDAC6 on immune activation, we tested the mRNA levels of proinflammatory cytokines (*IL1A*, *IL1B*, and *IL6*) and chemokines (*CCL2* and *CXCL10*) at 12, 16, 20, and 24 weeks. In HDAC6$^{+/y}$ mice, proinflammatory cytokine and chemokine levels were maximally induced (6.7-fold) at 16 weeks. Strikingly, genetic ablation of HDAC6 completely inhibited *IL1A* induction at 16, 20, and 24 weeks (Figure 8A). In both HDAC6$^{+/y}$ and HDAC6$^{-/y}$ livers, *IL1B* was notably induced (45.7-fold for HDAC6$^{+/y}$ and 38.9-fold for HDAC6$^{-/y}$) at 20 weeks, but genetic ablation of HDAC6 significantly decreased *IL1B* mRNA levels at 16 and 24 weeks (Figure 8B). *IL6* levels were also significantly reduced in HDAC6$^{-/y}$ livers at 16 and 24 weeks (Figure 8C). *CCL2* and *CXCL10* mRNA levels were slightly increased in HDAC6$^{-/y}$ mice compared with those in HDAC6$^{+/y}$ mice. *CCL2* mRNA levels were increased 29.2-fold in HDAC6$^{+/y}$ mice, but not in HDAC6$^{-/y}$ mice, at 16 weeks (Figure 8D). Histone deacetylase 6ablation significantly reduced *CXCL10* mRNA levels at 16, 20, and 24 weeks (Figure 8E).

To address which cell types are responsible for HDAC6-dependent immune activation, we isolated HCs, hepatic stellate cells (HSC), and Kupffer cells (KC) from 6-month-old HDAC6$^{+/y}$ and HDAC6$^{-/Y}$ mouse liver and showed that HSC and KC are the main sources of all tested cytokines and chemokines that were reduced in HDAC6$^{-/Y}$ liver except for *IL1A* in HSC (Figure S4A-J). In addition, protein levels of acetyl-K120 and -K320 p53 were increased in isolated HC, HSC, and KC from HDAC6$^{-/y}$ liver (Figure S4H). To investigate the role of p53 acetylation, we transfected wild-type, K120Q, and K320Q (K120Q and K320Q) of p53 into RAW 264.7 macrophage cells and checked the expression of cytokines (*IL1A*, *IL1B*, *IL6*) and chemokines (*CCL2*, *CXCL10*) (Figure S5). Although we observed that *IL6* and *CCL2* expression is reduced by p53, none of the acetylation mimic mutants of p53 (K120Q and K320Q) made meaningful differences compared with wild-type p53 (Figure S5C-D). *IL1A*, *IL1B*, and *CXCL10* expressions were not significantly changed by p53 overexpression (Figure S5A,B,E).

To search for an alternative pathway rather than p53, we performed DAVID-based functional annotation analysis using the same transcriptome data and observed changes in innate immunity–related gene expression in HDAC6$^{-/y}$ (Figure S3C). Previously, we and others showed that HDAC6 deacetylates Rig-I/Ddx58 to control innate immune responses.[20,21] Thus, we performed network analysis with Rig-I/Ddx58 and showed that Bst2, Oas1g, and Ly96 were significantly reduced in HDAC6$^{-/y}$ liver after multiple DEN treatments and closely related to Rig-I/Ddx58 (Figure 3D). Finally, we showed that the number of F4/80 positive macrophages in both tumor nodules and nontumorous

parenchyma is reduced in HDAC6$^{-/y}$ liver at 24 weeks with multiple DEN treatments (Figure 8F,G). Together, the genetic ablation of HDAC6 suppressed innate immune activation after multiple DEN treatments.

4 | DISCUSSION

Histone deacetylase 6, a unique member of the class IIb HDAC family, has emerged as a privileged target for cancer therapy because of its various effects on cancer-associated biological phenomena such as apoptosis, cell motility, inflammation, angiogenesis, and autophagy.[12,20,22-25] Most studies have been based on pharmaceutical inhibition of HDAC6 rather than genetic ablation for the development of anticancer drugs, and two HDAC6-specific inhibitors, ACY-1215 and ACY-241, have entered phase II clinical trials.[26] Whole-body HDAC6 knockout mice are viable and develop normally,[27] which has increased hope for the development of anticancer drugs without side effects. Notably, we and others have reported that genetic ablation of HDAC6 in mice leads to immune suppression and obesity,[20,28-30] emphasizing the intricate roles of HDAC6 in hepatocellular carcinogenesis.

Regeneration and tumorigenesis share common molecular pathways, and p53 is considered a crucial regulatory molecule that prevents regeneration from shifting into carcinogenesis.[31] Liver regeneration after two-thirds PHx in rodents has been considered a reliable animal model to test the regenerative proliferation of HCs without severe liver damage and inflammation.[32] Interestingly, we found that HDAC6$^{-/y}$ mice showed a similar regenerative liver growth as HDAC6$^{+/y}$ mice (Figure 3B) but, in contrast, significant reduction of HC proliferation at 48 hours after two-thirds PHx, (Figure 3E,F) suggesting nonproliferative regeneration in HDAC6$^{-/y}$ mouse liver. In transcriptome analysis using multiple DEN–treated liver samples, we found a significant downregulation of genes related to mitosis, cell division, and kinetochore organization, suggesting a mitotic failure (Figure 7, Figure S3). Of note, a significant amount of HCs are polyploid (about 80%) in normal conditions.[15] Therefore, if the ploidy of HCs increases in HDAC6$^{-/y}$ livers, this may explain nonreplicative liver regeneration in HDAC6$^{-/y}$ livers after two-thirds PHx. We interestingly observed that polyploidy (4C, >8C) was increased in isolated HCs from HDAC6$^{-/y}$ liver compared with HDAC6$^{+/y}$ (Figure S2), suggesting a possibility that polyploid HCs undergo cell division without DNA replication in HDAC6$^{-/y}$ liver after PHx.

Whether HDAC6 plays an inhibitory[33] or promoting[34] role in HCC has been recently debated. Owing to the lack of evidence from HCC models using whole-body HDAC6 knockout mice, it is not clear whether HDAC6 inhibition has beneficial effects on HCC patients. To investigate the role of HDAC6 in HCC progression, we employed three independent HCC mouse models with DEN + HFD, DEN + TAA, and multiple DEN treatments. In contrast to its inhibitory effect on hepatic cancer cell proliferation (Figure 2A and Figure 7F), genetic ablation of HDAC6 did not inhibit HCC but rather slightly enhanced HCC in two independent mouse models, DEN + HFD (Figure 4) and DEN + TAA (Figure 5). Importantly, whole-body HDAC6 ablation significantly promoted tumorigenesis in the multiple DEN treatment HCC model, emphasizing the role of HDAC6 as a tumor suppressor (Figure 6). These results indicated that whole-body HDAC6 knockout did not show an antitumoral effect and instead enhanced HCC development, especially in the multiple DEN treatment HCC model, supporting previous findings that HDAC6 plays a tumor-suppressing role in HCC.[33,35,36]

We and others recently reported that HDAC6 ablation in mice leads to the suppression of the innate immune response,[20,21] which plays a crucial role in tumor immunosurveillance and generation of antitumor immune responses.[37] From this perspective, we also showed that HDAC6 ablation leads to a general decrease in the mRNA levels of inflammatory cytokines (*IL1A*, *IL1B*, and *IL6*) and chemokines (*CCL2* and *CXCL10*) in the HCC model treated with multiple DEN, which was correlated with the promotion of HCC. Importantly, we showed that the number of F4/80 positive macrophages in both tumor nodules and nontumorous parenchyma is reduced in HDAC6$^{-/y}$ liver at 24 weeks with multiple DEN treatments (Figure 8F,G). These suggest that whole-body HDAC6 ablation can lead to imperfections in the innate immune response against HCC. However, acetylation mimic mutants (K120Q and K320Q) of p53 did not make meaningful differences in the expression of cytokines (*IL1A*, *IL1B*, *IL6*) and chemokines (*CCL2*, *CXCL10*) (Figure S5), suggesting an alternative pathway. DAVID-based functional annotation analysis showed changes in innate immunity-related gene expression in HDAC6$^{-/y}$ (Figure S3C). Previously, we and others showed that HDAC6 deacetylates Rig-I/Ddx58 to control innate immune responses.[38,39] Network analysis with Rig-I/Ddx58 revealed that Bst2, Oas1g, and Ly96 were significantly reduced in HDAC6$^{-/y}$ liver after DEN treatment and closely related to Rig-I/Ddx58 (Figure S3D). Therefore, Rig-I would be a possible target of HDAC6 in HCC development, which is worth exploring further.

In summary, contrary to the general assumption that HDAC6 inhibition leads to hyperacetylation of p53, resulting in tumor suppression, our data from in vivo animal HCC models emphasize the importance of multiple roles of HDAC6 in hepatocellular carcinogenesis, highlighting its immunosuppressive effects.

AUTHOR CONTRIBUTIONS

Sophors Phorl, Azra Memon: Designed and performed experiments, analyzed data, drafted manuscript. Yuri Seo, Hoang Thi Oanh, Tran Trung Nghia, Nguyen Le Minh Tri, Chang Hoon Lee: Performed experiments, analyzed data, revised manuscript. Woon Kyu Lee, Joo-Yong Lee: Designed experiments, analyzed data, revised manuscript.

ACKNOWLEDGEMENTS

This work was supported by the National Research Foundation of Korea (NRF) 2019R1A2C1005334, 2016M3A9E1918314, the Ministry of Health & Welfare, Republic of Korea (grant number: HI21C1503), and the Commercialization Promotion Agency for R&D Outcomes (COMPA) funded by the Ministry of Science and ICT (MSIT) [CNU(2021)-011, R&D Equipment Engineer Education Program].

DISCLOSURE

The authors have no conflict of interest.

ETHICS STATEMENT

Animal studies and all experimental procedures: Approval and guidelines of the INHA Institutional Animal Care and Use Committee (INHA IACUC) of the Medical School of Inha University (INHA 160901–435–1).

ORCID

Joo-Yong Lee https://orcid.org/0000-0003-1049-6006

REFERENCES

1. Rui L. Energy metabolism in the liver. *Compr Physiol*. 2014;4:177-197.
2. Degasperi E, Colombo M. Distinctive features of hepatocellular carcinoma in non-alcoholic fatty liver disease. *Lancet Gastroenterol Hepatol*. 2016;1:156-164.
3. Forner A, Llovet JM, Bruix J. Hepatocellular carcinoma. *Lancet*. 2012;379:1245-1255.
4. Mu X, Espanol-Suner R, Mederacke I, et al. Hepatocellular carcinoma originates from hepatocytes and not from the progenitor/biliary compartment. *J Clin Invest*. 2015;125:3891-3903.
5. Henderson JM, Polak N, Chen J, et al. Multiple liver insults synergize to accelerate experimental hepatocellular carcinoma. *Sci Rep*. 2018;8:10283.
6. Brown ZJ, Heinrich B, Greten TF. Mouse models of hepatocellular carcinoma: an overview and highlights for immunotherapy research. *Nat Rev Gastroenterol Hepatol*. 2018;15:536-554.
7. Hafner A, Bulyk ML, Jambhekar A, Lahav G. The multiple mechanisms that regulate p53 activity and cell fate. *Nat Rev Mol Cell Biol*. 2019;20:199-210.
8. Kastenhuber ER, Lowe SW. Putting p53 in context. *Cell*. 2017;170:1062-1078.
9. Park SY, Phorl S, Jung S, et al. HDAC6 deficiency induces apoptosis in mesenchymal stem cells through p53 K120 acetylation. *Biochem Biophys Res Commun*. 2017;494:51-56.
10. Ding G, Liu HD, Huang Q, et al. HDAC6 promotes hepatocellular carcinoma progression by inhibiting P53 transcriptional activity. *FEBS Lett*. 2013;587:880-886.
11. Ryu HW, Shin DH, Lee DH, et al. HDAC6 deacetylates p53 at lysines 381/382 and differentially coordinates p53-induced apoptosis. *Cancer Lett*. 2017;391:162-171.
12. Lee YS, Lim KH, Guo X, et al. The cytoplasmic deacetylase HDAC6 is required for efficient oncogenic tumorigenesis. *Cancer Res*. 2008;68:7561-7569.
13. Park SY, Phorl S, Jung S, et al. HDAC6 deficiency induces apoptosis in mesenchymal stem cells through p53 K120 acetylation. *Biochem Biophys Res Comm*. 2017;494:51-56.
14. Zhao Y, Lu S, Wu L, et al. Acetylation of p53 at lysine 373/382 by the histone deacetylase inhibitor depsipeptide induces expression of p21Waf1/Cip1. *Mol Cell Biol*. 2006;26:2782-2790.
15. Zhang S, Lin YH, Tarlow B, Zhu H. The origins and functions of hepatic polyploidy. *Cell Cycle*. 2019;18:1302-1315.
16. Park EJ, Lee JH, Yu G-Y, et al. Dietary and genetic obesity promote liver inflammation and tumorigenesis by enhancing IL-6 and TNF expression. *Cell*. 2010;140:197-208.
17. Salomao M, Remotti H, Vaughan R, Siegel AB, Lefkowitch JH, Moreira RK. The steatohepatitic variant of hepatocellular carcinoma and its association with underlying steatohepatitis. *Hum Pathol*. 2012;43:737-746.
18. Memon A, Pyao Y, Jung Y, Lee JI, Lee WK. A modified protocol of diethylnitrosamine administration in mice to model hepatocellular carcinoma. *Int J Mol Sci*. 2020;21:5461.
19. Zhang WB, Zhang HY, Jiao FZ, Wang LW, Zhang H, Gong ZJ. Histone deacetylase 6 inhibitor ACY-1215 protects against experimental acute liver failure by regulating the TLR4-MAPK/NF-κB pathway. *Biomed Pharmacother*. 2018;97:818–824.
20. Choi SJ, Lee HC, Kim JH, et al. HDAC 6 regulates cellular viral RNA sensing by deacetylation of RIG-I. *EMBO J*. 2016;35:429-442.
21. Liu L, Zhou X, Shetty S, Hou G, Wang Q, Fu J. HDAC6 inhibition blocks inflammatory signaling and caspase-1 activation in LPS-induced acute lung injury. *Toxicol Appl Pharmacol*. 2019;370:178-183.
22. Hubbert C, Guardiola A, Shao R, et al. HDAC6 is a microtubule-associated deacetylase. *Nature*. 2002;417:455-458.
23. Lee JY, Koga H, Kawaguchi Y, et al. HDAC6 controls autophagosome maturation essential for ubiquitin-selective quality-control autophagy. *EMBO J*. 2010;29:969-980.
24. Li Y, Shin D, Kwon SH. Histone deacetylase 6 plays a role as a distinct regulator of diverse cellular processes. *FEBS J*. 2013;280:775-793.
25. Kaluza D, Kroll J, Gesierich S, et al. Class IIb HDAC6 regulates endothelial cell migration and angiogenesis by deacetylation of cortactin. *EMBO J*. 2011;30:4142-4156.
26. Pulya S, Amin SA, Adhikari N, Biswas S, Jha T, Ghosh B. HDAC6 as privileged target in drug discovery: a perspective. *Pharmacol Res*. 2021;163:105274.
27. Zhang Y, Kwon S, Yamaguchi T, et al. Mice lacking histone deacetylase 6 have hyperacetylated tubulin but are viable and develop normally. *Mol Cell Biol*. 2008;28:1688-1701.
28. Magupalli VG, Negro R, Tian Y, et al. HDAC6 mediates an aggresome-like mechanism for NLRP3 and pyrin inflammasome activation. *Science*. 2020;369:eaas8995.
29. Qian H, Chen Y, Nian Z, et al. HDAC6-mediated acetylation of lipid droplet-binding protein CIDEC regulates fat-induced lipid storage. *J Clin Invest*. 2017;127:1353-1369.
30. Jung S, Han M, Korm S, et al. HDAC6 regulates thermogenesis of brown adipocytes through activating PKA to induce UCP1 expression. *Biochem Biophys Res Commun*. 2018;503:285-290.
31. Charni M, Aloni-Grinstein R, Molchadsky A, Rotter V. p53 on the crossroad between regeneration and cancer. *Cell Death Differ*. 2017;24:8-14.
32. Michalopoulos GK. Liver regeneration after partial hepatectomy: critical analysis of mechanistic dilemmas. *Am J Pathol*. 2010;176:2-13.
33. Yang HD, Kim HS, Kim SY, et al. HDAC6 suppresses Let-7i-5p to Elicit TSP1/CD47-mediated anti-tumorigenesis and phagocytosis of hepatocellular carcinoma. *Hepatology*. 2019;70:1262-1279.
34. Qiu W, Wang B, Gao Y, et al. Targeting histone deacetylase 6 reprograms interleukin-17-producing helper T cell pathogenicity and facilitates immunotherapies for hepatocellular carcinoma. *Hepatology*. 2020;71:1967-1987.
35. Jung KH, Noh JH, Kim JK, et al. Histone deacetylase 6 functions as a tumor suppressor by activating c-Jun NH2-terminal kinase-mediated beclin 1-dependent autophagic cell death in liver cancer. *Hepatology*. 2012;56:644-657.
36. Bae HJ, Jung KH, Eun JW, et al. MicroRNA-221 governs tumor suppressor HDAC6 to potentiate malignant progression of liver cancer. *J Hepatol*. 2015;63:408-419.
37. Demaria O, Cornen S, Daeron M, Morel Y, Medzhitov R, Vivier E. Harnessing innate immunity in cancer therapy. *Nature*. 2019;574:45-56.
38. Choi SJ, Lee HC, Kim JH, et al. HDAC6 regulates cellular viral RNA sensing by deacetylation of RIG-I. *EMBO J*. 2016;35:429-442.

39. Liu HM, Jiang F, Loo YM, et al. Regulation of retinoic acid inducible gene-I (RIG-I) activation by the histone deacetylase 6. *EBioMedicine*. 2016;9:195-206.

SUPPORTING INFORMATION

Additional supporting information can be found online in the Supporting Information section at the end of this article.

How to cite this article: Phorl S, Memon A, Seo Y, et al. Opposing roles of HDAC6 in liver regeneration and hepatocarcinogenesis. *Cancer Sci*. 2022;113:2311–2322. doi:10.1111/cas.15391